



## A voltammetric study on the atomic layer deposition of selenium and antimony on platinum electrode

Yuan Chen, Huicheng Huang, Zhishun Weil, Ying Chang, Annie Pradel,  
Pascal Boulet, M. -C. Record

### ► To cite this version:

Yuan Chen, Huicheng Huang, Zhishun Weil, Ying Chang, Annie Pradel, et al.. A voltammetric study on the atomic layer deposition of selenium and antimony on platinum electrode. 17th International Conference on Sustainable Energy Technologies, Aug 2018, WUHAN, China. pp.219-228. hal-03572049

**HAL Id: hal-03572049**

**<https://hal.science/hal-03572049>**

Submitted on 14 Feb 2022

**HAL** is a multi-disciplinary open access archive for the deposit and dissemination of scientific research documents, whether they are published or not. The documents may come from teaching and research institutions in France or abroad, or from public or private research centers.

L'archive ouverte pluridisciplinaire **HAL**, est destinée au dépôt et à la diffusion de documents scientifiques de niveau recherche, publiés ou non, émanant des établissements d'enseignement et de recherche français ou étrangers, des laboratoires publics ou privés.

# A VOLTAMMETRIC STUDY ON THE ATOMIC LAYER DEPOSITION OF SELENIUM AND ANTIMONY ON PLATINUM ELECTRODE

Yuan CHEN<sup>1,2,3</sup>, Huicheng HUANG<sup>1,2,3</sup>, Zhishun WEI<sup>1,2,3</sup>, Ying CHANG<sup>1,2,3</sup>, Annie PRADEL<sup>4</sup>,  
Boulet PASCAL<sup>5,6</sup>, Marie-Christine RECORD<sup>5,7,\*</sup>

<sup>1</sup> Hubei Provincial Key Laboratory of Green Materials for Light Industry, Hubei University of Technology, Wuhan, Hubei 430068, China

<sup>2</sup> Collaborative Innovation Center of Green Light-weight Materials and Processing, Hubei University of Technology, Wuhan, Hubei 430068, China

<sup>3</sup> School of Materials and Chemical Engineering, Hubei University of Technology, Wuhan, Hubei 430068, China

<sup>4</sup> CNRS, ICGM UMR 5253, ChV, CC1503, Université de Montpellier, F-34095, France

<sup>5</sup> Aix Marseille Univ, F-13397 Marseille 20, France

<sup>6</sup> CNRS, MADIREL UMR 7246, F-13397 Marseille 20, France

<sup>7</sup> CNRS, IM2NP UMR 7334, F-13397 Marseille 20, France, m-c.record@univ-amu.fr

**Abstract:** The present paper is a detailed study on the atomic layer deposition of selenium and antimony on platinum electrode by electrochemical atomic layer epitaxy (EC-ALE). Voltammetry and coulometry experiments were performed in this work to investigate the electrochemical behaviors of selenium and antimony on the polycrystalline platinum electrode. The results show that on Pt substrates Se ions can directly form a UPD layer with full coverage without the formation of bulk Se. The total Faradaic charge of the UPD Se is calculated to be  $924 \mu\text{C cm}^{-2}$ . A Pt electrode adsorbed irreversibly with  $\text{SbO}^+$  species is obtained by introducing the fresh Sb solution continuously into the electrochemical cell. The irreversibly adsorbed  $\text{SbO}^+$  species begin to desorb when the potential is more positive than 0.50 V. The reduction potential of irreversibly adsorbed  $\text{SbO}^+$  to metallic Sb atoms amounts to 0.11 V. After the irreversibly adsorbed  $\text{SbO}^+$  species are reduced to metallic Sb, Sb atoms can be further deposited onto this Sb-modified Pt electrode in the way of UPD to increase the coverage of the metallic Sb monolayer. The UPD potential of antimony on the Sb-modified Pt electrode amounts to  $-0.07$  V. Finally, a Sb monolayer with the depositing charge  $981 \mu\text{C cm}^{-2}$  is obtained. Now the alternative deposition of Sb-Se compound by EC-ALE method is under study.

**Keywords:**  $\text{Sb}_2\text{Se}_3$ ; Electrochemistry deposition; EC-ALE; Atomic layer; absorption;

## 1. INTRODUCTION

$\text{Sb}_2\text{Se}_3$ , a member of V-VI group semiconductors, is the unique intermediate compound in the Sb-Se equilibrium phase diagram (GHOSH, 1993: 753).  $\text{Sb}_2\text{Se}_3$  is a semiconductor with a layered crystal structure (space group  $\text{Pnma}$ ;  $n^\circ 62$ ) in which each Sb atom and each Se atom is bound to three atoms of the opposite kind that are held together by weak secondary bonds (MADELUNG, 1992: 446). Not only does  $\text{Sb}_2\text{Se}_3$  itself be a fine thermoelectric material at room temperature (with Seebeck coefficients of 46.2 and 18.3  $\mu\text{V/K}$  for the polycrystalline and amorphous  $\text{Sb}_2\text{Se}_3$  thin films (RAJPURE, 1999: 1079)), but it is also an important component of the solid solutions  $(\text{Bi}, \text{Sb})_2(\text{Te}, \text{Se})_3$ , which are regarded as the best and, in fact, the only materials used for cooling (XIAO, 2006: 25). In addition, it also has promising applications in several other fields such as optoelectronic, photovoltaic and batteries. Consequently, both elaboration and characterization of this compound have been largely studied (see for example Ref. (FERNÁNDEZ, 2000: 202; RAJPURE, 1999: 1079; XUE, 2008: 351; YU, 2010: 1258; WANG, 2013: 1)).

Miniaturization of the devices requires the use of thin films which are usually prepared by physical vapor deposition methods. In our previous work (CHEN, 2015: 2399), a thin film of  $\text{Sb}_2\text{Se}_3$  compound was obtained successfully on polycrystalline gold electrode via the route of Electrochemical Atomic Layer Epitaxy (EC-ALE) technique, which was put forward by J. Stickney (GREGORY, 1991: 543) and was proved to be a valid approach to control these parameters for the deposition of chalcogenide compounds on metallic substrates (LISTER, 1996: 153; ZHU, 2005: 5465; FORESTI, 2005: 6900; CHEN, 2015: 2399). This method is based on the alternate underpotential deposition (UPD) of atomic layers of the elements that form the compound, in a cycle that can be repeated as many times as desired. The major advantage of this method is that the individual steps of each cycle can be investigated and optimized independently.

It is generally known that the substrate plays an important role in the process of electrodeposition. Therefore, to study how the substrates of different materials affect the processes of underpotential deposition is very important and significative. Platinum has always been of particular interest owing to its electrocatalytic properties and is also widely used as the material of substrates in the studies of electrodeposition. However, in the field of EC-ALE, only a few studies utilized Pt as the substrates, which respectively reported the EC-ALE of  $\text{Sb}_2\text{Te}_3$  (YANG, 2006: 4599),  $\text{Bi}_2\text{Te}_3$  (ZHU, 2005: 4041) and  $\text{Bi}_2\text{Se}_3$  (XIAO, 2009: 6821) on Pt electrodes. As we know so far, there is no result reported in the literature concerning the electrodeposition of  $\text{Sb}_2\text{Se}_3$  thin film on Pt electrode by EC-ALE method.

This paper, as a preliminary study, is devoted to investigating the atomic layer deposition of selenium and antimony on the polycrystalline platinum electrode and to provide the electrodeposition parameters for the subsequent alternate EC-ALE process. The irreversible adsorption and reversible underpotential deposition (UPD) behaviors of Sb on Pt electrode are studied in detail because they have not yet been fully understood according to the literature so far and they affect the obtaining of the high-coverage Sb atomic layer. In this work, the electrochemical behaviors of Sb and Se on the polycrystalline Pt electrode are studied by means of cyclic voltammetry and coulometry. Thanks to the flexibility of the EC-ALE equipment, the work led to a better understanding on the electrochemical behavior of Sb on Pt electrode. A method to obtain a metallic Sb monolayer with higher coverage on Pt electrode was determined. Now the alternative deposition of Sb-Se compound by EC-ALE method is under study.

## 2. EXPERIMENTAL

### 2.1. Solutions and Chemicals

Solutions are prepared using ACS reagent grade or higher-grade chemicals (Sigma-Aldrich, Inc., USA) and deionized water (Milli-Q 18.2  $\text{M}\Omega\cdot\text{cm}$ , Merck KGaA, Darmstadt, Germany). Three different solutions are used in this study. The antimony solutions contain 0.05 mM  $\text{Sb}_2\text{O}_3$  (99.999%) as reactant and 0.2 M  $\text{Na}_2\text{SO}_4$  as supporting electrolyte. The pH of these solutions is 1.0. The selenium solutions consist of  $\text{SeO}_2$  (99.999%) and  $\text{Na}_2\text{SO}_4$ , at pH 1.0, with concentration of 0.5 mM and 0.2 M, respectively. Supporting electrolyte solutions, with same pH and ionic strength as the deposition solutions, are used as blank solutions to rinse the cell. The pH values of the solutions are adjusted with  $\text{H}_2\text{SO}_4$ . Just before the beginning of each series of measurements, all the solutions are freshly prepared and then degassed for 30 min with high purity Ar gas (Ar Bip,  $\text{O}_2 < 10$  ppb, Air Products and Chemicals, Inc., France), which is bubbled into the solution. All experiments are performed at room temperature with solution maintained under Ar atmosphere.

### 2.2. Substrates

Platinum substrates are used as working electrodes. They consist of quartz slides, coated with 200 nm thick platinum films (99.9% pure) by electron beam physical vapor deposition. Under the Pt film, a thin layer of Cr (25 nm) is deposited to improve adhesion of platinum onto quartz. The platinum substrates are pretreated as follows: they are firstly annealed at 375  $^\circ\text{C}$  for 18 h at  $10^{-6}$  Torr in sealed glass tubes and then soaked in hot nitric acid for 5 min. Before each experiment, cyclic voltammetry (CV) scanning (repeated 25 times) of the Pt substrate in 0.1 M

H<sub>2</sub>SO<sub>4</sub> solution is performed with potential scan from -0.27 to 1.20 V to clean and check the substrate. The CV curve of the Pt electrode in 0.1 M H<sub>2</sub>SO<sub>4</sub> is shown in Figure 1.

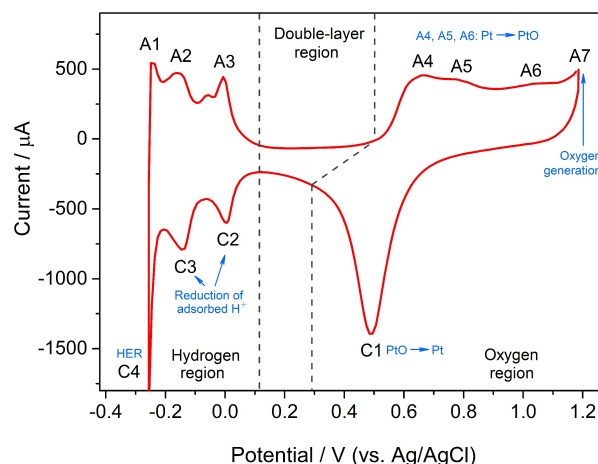


Figure 1: Cyclic voltammogram of the Pt electrode in 0.1 M H<sub>2</sub>SO<sub>4</sub>. The scanning rate is 100 mV/s.

In Figure 1, three potential regions may be defined from the CV of Pt, i.e. the oxygen region (0.50 to 1.20 V), the double layer region (0.12 to 0.50 V) and the hydrogen region (-0.27 to 0.12 V). In the oxygen region, the anodic peaks A4, A5 and A6 correspond to the oxidation of the platinum to PtO (JERKIEWICZ, 2004: 1451), while the cathodic peak C1 corresponds to the reduction of PtO to Pt. The potential where peak A7 appears corresponds to the beginning of the oxygen generation. In the hydrogen region, the peaks C2 and C3 correspond to the reduction of a monolayer of adsorbed hydrogen ions, while the peaks A2 and A3 correspond to its oxidative desorption. By integrating the peaks C2 and C3 in corresponding I-t curve of CV, the electric charge of the adsorbed hydrogen is calculated to be 796  $\mu\text{C}$  after deducting the charge of double layer. Thus, the real area of the Pt electrode is estimated to be 3.79 cm<sup>2</sup> by taking the value of 210  $\mu\text{C cm}^{-2}$  as reference (TRASATTI, 1991: 353). The peaks C4 and A1 correspond to the generation and oxidation of hydrogen respectively.

### 2.3. Electrochemical Testing Equipment

All electrochemical experiments are performed with the EC-ALE equipment developed by us and depicted in our previous work (CHEN, 2014: 55; CHEN, 2015: 2399). The electrochemical flow cell is close to those described by the Stickney (FLOWER, 2002: 273) and Zhu-Yang (ZHU, 2005: 4041) working groups. A platinum sheet (Sigma-Aldrich, Inc., USA) is used as counter electrode in the electrochemical cell. All electrochemical potential values are measured with respect to the potential of an Ag/AgCl electrode (3.0 M NaCl, 0.209 V vs. standard hydrogen electrode (SHE), AMETEK, Inc., USA) as a reference. The atomic layer deposition of Se and Sb elements was studied electrochemically by means of cyclic voltammetry and coulometry.

## 3. RESULTS AND DISCUSSION

### 3.1. Selenium Electrochemical Behavior on Pt

Figure 2a and Figure 2b show the cyclic voltammetry (CV) curves of the polycrystalline Pt electrode in 0.5 mM SeO<sub>2</sub> + 0.2 M Na<sub>2</sub>SO<sub>4</sub> solution (pH 1.0), successively scanned from 1.06 V to various potential limits (see curve legend in the figures) at a scanning rate of 20 mV/s. As the cathodic scan limit moves from 0.55 V to 0.30 V, a reductive peak C1 (at 0.48 V) and two oxidative peaks A3 (at 0.90 V) and A2 (at 0.74 V) appear successively. The current density of peak A3 reaches its limit when the cathodic scan limit is 0.3 V. The peak A2 seems to keep on increasing when the cathodic scan limit moves further to 0.10 V. However, one can find from Figure 2b that the peak A2 has reached its limit. The increasing of peak A2 in Figure 2a during the cathodic scan limit moves from 0.30 V to 0.10 V should be due to the overlapping by peak A1. Consequently, the reductive peak C1 and oxidative peaks A3 and A2 are associated with the UPD of Se and its anodic stripping, which corresponds to the reaction Equation 1.



The total integrated Faradaic charge of the anodic stripping peaks A3 and A2 is 924  $\mu\text{C cm}^{-2}$ , which is near to the value of 910  $\mu\text{C cm}^{-2}$ , the stripping charge density of Se UPD layer and oxidation of surface Pt, as reported by Santos and Machado (SANTOS, 2004: 203). The same experiment processing and voltammetric phenomena between this study and the literature (SANTOS, 2004: 203) indicate that the Se deposition of peak C1 is close to

one UPD layer. Compared with the results in our previous paper (CHEN, 2015: 2399) about the electrochemical behaviors of Se on Au, one can find that on Pt substrates Se ions can directly form a total UPD layer without the formation of bulk Se, suggesting that in kinetics the UPD process of Se is faster on Pt substrates than that on Au substrates. This also indicates that to form a total UPD layer on Pt substrate a rinsing process for cleaning the redundant bulk Se is needless. The results above prove that Se element has different UPD behaviors on the substrates of different materials.

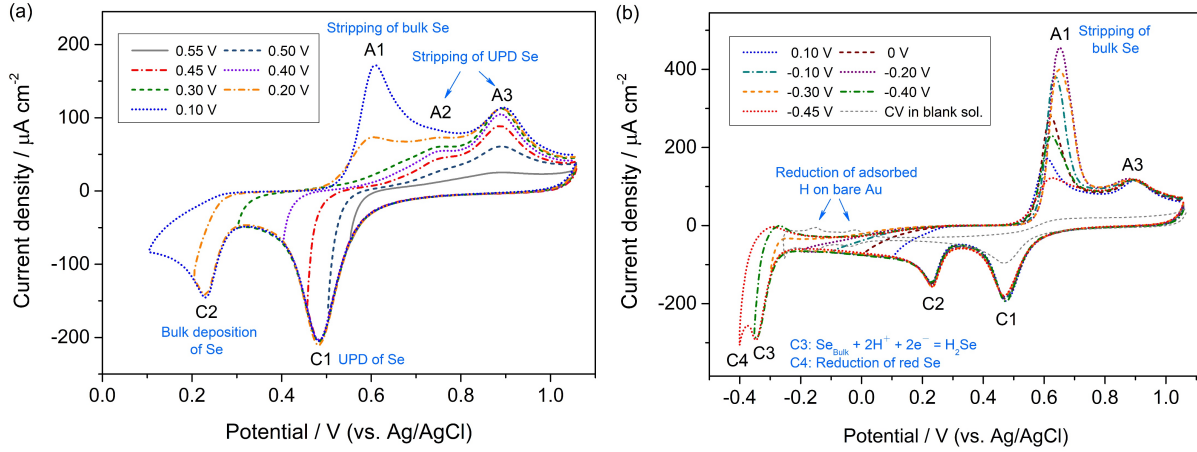
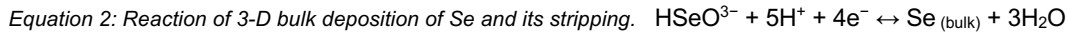
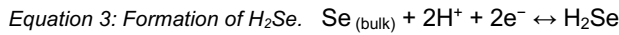


Figure 2: Cyclic voltammograms of Pt electrode in a 0.5 mM  $\text{SeO}_2$  + 0.2 M  $\text{Na}_2\text{SO}_4$  solution (pH 1.0). The cathodic potential limits are: (a) 0.55 V, 0.50 V, 0.45 V, 0.40 V, 0.30 V, 0.20 V and 0.10 V; (b) 0.10 V, 0 V, -0.10 V, -0.20 V, -0.30 V, -0.40 V and -0.45 V, respectively. Used as control, the gray dashed curve in (b) is the cyclic voltammogram of Pt electrode in blank solution with the scanning potential from 1.06 V to -0.26 V. The scanning rate is 20 mV/s.

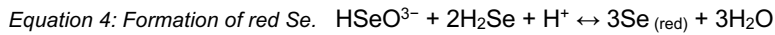
When the electrode is further scanned negatively to 0.20 V, an additional reductive peak C2 and an oxidative stripping peak A1 appear. As the cathodic scan limit moves more negatively, the oxidative stripping peak A1 continually increases and reaches a maximum when the cathodic scan limit is -0.20 V, indicating the peak C2 corresponds to the 3-D bulk deposition of Se and the peak A1 corresponds to its stripping, which corresponds to the reaction Equation 2.



When the cathodic limit of cyclic voltammetry scanning is more negative than -0.20 V, an additional reduction peak C3 is observed at -0.34 V. Furthermore, A1, the stripping peak of bulk Se, decreases with the moving towards more negative cathodic limits. As already discussed in our previous work (CHEN, 2015: 2399), the C3 peak should correspond to the reduction of bulk Se to  $\text{H}_2\text{Se}$ , which is soluble. The reaction is shown as Equation 3.



The reductive stripping of bulk Se leads to the decrease of the A1 peak. Similar as the situation discussed in the previous work (CHEN, 2015: 2399) on Au electrode, once  $\text{H}_2\text{Se}$  is formed, the two species  $\text{HSeO}_3^-$  and  $\text{H}_2\text{Se}$  coexist in the cell and lead to a subsequent chemical reaction (Equation 4) by which red Se is formed. The last cathodic peak C4 should correspond to the further reduction of the red Se.



The gray dashed curve in Figure 2b, used as control, is the cyclic voltammogram of Pt electrode in blank solution with the scanning potential from 1.06 V to -0.26 V with the same scanning rate. It is worthwhile to note the following two details: (i) the reductive peak of PtO locates at the same position as the peak C1, indicating that the peak C1 is actually the overlapping of the reductive peak of PtO and the UPD peak of Se, and this observation coincides with the literature (SANTOS, 2004: 203); (ii) in the CV curves of Pt electrode in Se solution, the reductive peaks of adsorbed hydrogen ions (see the peaks C2 and C3 in Figure 1) are not observed. The reason is that before entering hydrogen region, the Pt electrode is already covered by UPD and bulk Se, without bare Pt exposed to the solution, thus the characteristic reductive peaks of adsorbed hydrogen cannot be observed.

### 3.2. Antimony Electrochemical Behavior on Pt

In the current electrochemistry, there are two methods to form atomic monolayers of various metals: the underpotential deposition method and the immersion method (HERRERO, 1994: 101; JUNG, 1997: 277; WU, 2000:

3683). The principles of both methods are distinguished from each other. In the underpotential deposition method, a simple immersion of an electrode into a solution does not lead to any interaction between the depositing species and the electrode surface. To induce an interaction, a cathodic potential is generally applied, and the surface concentration of the deposited element is determined by the applied potential. In the immersion method, on the contrary, a strong or irreversible adsorption of a depositing species is achieved upon immersion, and the surface concentration of the deposited species is determined by the contact time and the concentration of the adsorbing species. Since the irreversibly adsorbed species generally retains its oxidation state in solution, an application of a cathodic potential is needed to reduce the adsorbate to the metallic element.

In our previous work (CHEN, 2015: 2399), when the working electrodes are Au substrates, the irreversible adsorption of Sb species in solutions ( $\text{SbO}^+$ ) also happens. However, the irreversible adsorption process on Au substrate is completed immediately when the Sb solution is introduced into the electrochemical cell. This can be proved by the observation that the OCV (open circuit voltage) reaches a stable value in a very short time (less than 1 s). In addition, the reductive peak of the irreversibly adsorbed  $\text{SbO}^+$  usually hides in the UPD peak of Sb when the potential of the Au electrode is scanned negatively in Sb solution (YAN, 2004: 843). Therefore, in the EC-ALE studies that focus on obtaining the metallic Sb monolayer of full coverage on Au substrates, usually the irreversible adsorption process is not discussed separately.

However, the irreversible adsorption process of Sb species on Pt electrode is quite slow in kinetics. Thus, in EC-ALE study, the irreversible adsorption behavior of Sb on Pt electrode should be investigated separately because the amount of irreversibly adsorbed Sb species will affect the subsequent UPD process. J.M. Feliu et al. (HERRERO, 1994: 101; FELIU, 1988: 149), M.J. Weaver et al. (KIZHAKEVARIAM, 1994: 183) and S.G. Sun et al. (WU, 2000: 277; SUN, 1990: 205) studied the irreversible adsorption behavior of Sb species by immersing simply Pt electrode in a solution containing  $\text{SbO}^+$  ions at the OCV, but these studies focused on the electrocatalytic properties of Sb modified Pt electrode towards the oxidative reaction of a variety of organic molecules. In these literatures, the Pt electrode was not fully covered by Sb atoms because only the irreversible adsorption process was involved, but not combined with the UPD process. As we know so far, the method of obtaining a metallic Sb monolayer of full coverage on Pt electrode has not been previously reported. In this section, the irreversible adsorption process of Sb on Pt electrode was firstly studied. Subsequently, the UPD behavior of Sb on the Pt electrode, which was pre-adsorbed by Sb was investigated.

#### *Irreversible Adsorption Behavior of Sb on Pt Electrode*

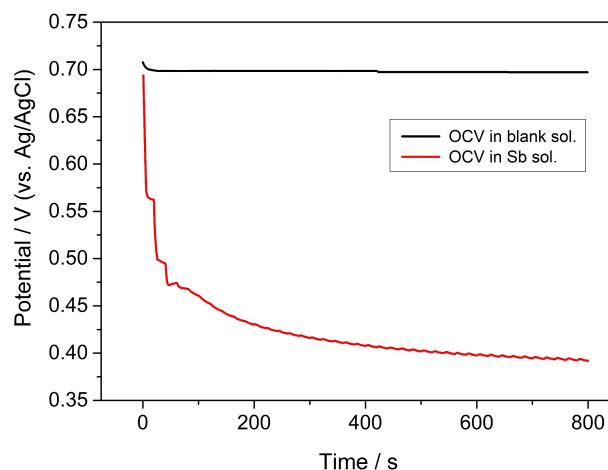


Figure 3. The varying of the OCV of Pt electrode during the irreversible adsorption process of Sb (red curve), where the Sb solution is introduced into the electrochemical cell; kept flowing for 5 s and then kept stable for 15 s as one cycle; totally 40 cycles are performed. The black curve shows the varying of the OCV of Pt electrode in a control experiment, where the blank solution is used instead of the Sb solution.

According to the literatures mentioned above (HERRERO, 1994: 101; FELIU, 1988: 149; KIZHAKEVARIAM, 1994: 183; WU, 2000: 277; SUN, 1990: 205), antimony can adsorb irreversibly on Pt surface by immersing simply Pt electrode in a solution containing  $\text{SbO}^+$  ions at the OCV. Two advantages of this irreversible adsorption may be stated as, (i) the coverage of  $\text{Sb}_{\text{ad}}$  can be easily controlled by the time of immersing and the concentration of the Sb solution; (ii) the  $\text{Sb}_{\text{ad}}$  modified Pt electrode can be studied in a solution free of  $\text{SbO}^+$  ions. In this study, the aim is to obtain a metallic Sb monolayer of full coverage on Pt electrode, so the first step is to obtain as much as possible the irreversibly adsorbed Sb species on Pt electrode. Thus, we design the following experimental procedure to adsorb adequate Sb species on a clean Pt electrode:

- (i) Before the beginning of the experiments, the clean Pt electrode is placed in the electrochemical cell filled with blank solution.
- (ii) The Sb solution is introduced into the electrochemical cell and kept flowing for 5 s. Then the Sb



solution is kept stable for 15 s. (iii) The step (ii) as a cycle is repeated totally for 40 times, and the varying of the OCV of Pt electrode during this process is shown as the red curve in Figure 3. (iv) As control, a similar experiment procedure is performed as steps (i) to (iii), but during the whole process the blank solution is used instead of the Sb solution. The varying of the OCV of Pt electrode during this process is shown as the black curve in Figure 3.

From the results shown in Figure 3, one can see that the OCV of Pt electrode decreases continuously in the Sb solution, indicating that Sb species ( $\text{SbO}^+$ ) are indeed adsorbed irreversibly on Pt electrode. Before the beginning of the experiments, the clean Pt electrode is kept in the electrochemical cell filled with blank solution, where the OCV is approximately 0.70 V. The high OCV is due to the chemical oxygen  $\text{O}_{\text{chem}}$  adsorbed on Pt electrode in an acid solution environment according to the literature (JERKIEWICZ, 2004: 1451). When the Sb solution is introduced into the cell, the  $\text{SbO}^+$  species are irreversibly adsorbed on Pt and replace the sites of adsorbed chemical oxygen  $\text{O}_{\text{chem}}$ , leading to the structural change of the double-layer on the surface of Pt electrode. The structural change of the double-layer leads to the change of OCV. Therefore, the decrease of the OCV demonstrates the occurring of the irreversible adsorption of Sb species.

The OCV of Pt electrode in Sb solution approximately reaches a plateau after 800 s (40 cycles), indicating that the amount of irreversibly adsorbed Sb species reaches a maximum. This observation also illustrates that the irreversible adsorption process of Sb species on Pt substrate is slow in kinetics, or in other words, the process of replacing  $\text{O}_{\text{chem}}$  by  $\text{SbO}^+$  species is slow in kinetics.

After the irreversible adsorption process of Sb species is achieved on Pt substrate, the next step is to study the redox properties of the adsorbed Sb species. The investigation is performed as follows, and for the sake of clarity, this experimental process is also shown as Figure 4a.

(i) After the irreversible adsorption process of  $\text{SbO}^+$  species is achieved on the Pt electrode, the cell is rinsed with blank solution for 25 s (from point A to B in Figure 4a), and during this time no potential is applied, the voltage showed between point A and B is the OCV. (ii) A cyclic voltammetry scanning is performed from the OCV for 7 cycles (after point B). The cathodic and anodic scanning limits are  $-0.26$  V and  $1.06$  V, respectively.

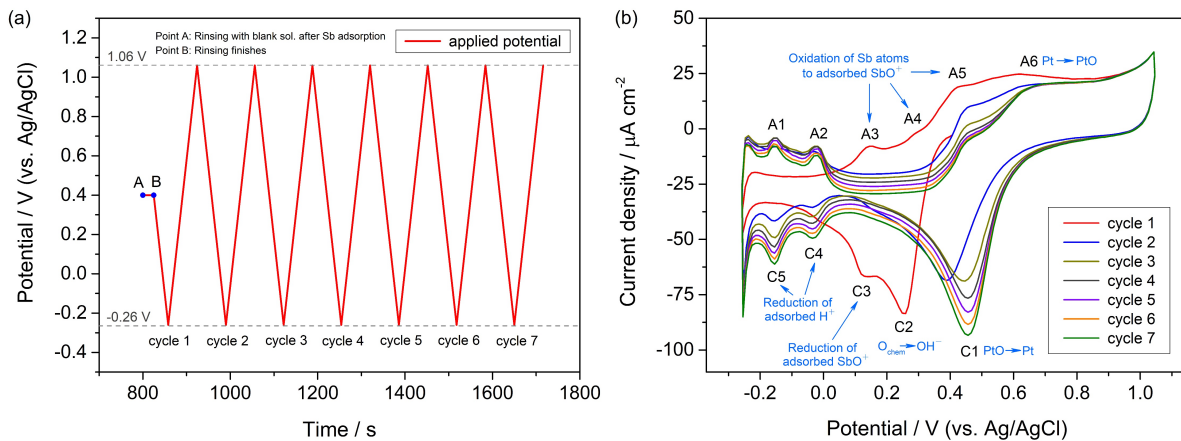


Figure 4: The cyclic voltammetry experiment of the Pt electrode (adsorbed with Sb species) in blank solution: (a) the experimental process and (b) the results of CV scanning. The scanning rate is 20 mV/s.

In Figure 4a, one can observe that the OCV keeps stable round 0.40 V during the rinsing process with blank solution (between point A and B), indicating that the adsorption process of Sb species is irreversible and the adsorbed species is stable on Pt substrate. Figure 4b shows the voltammograms of the Pt electrode (adsorbed with Sb species) in blank solution. The peak C1 corresponds to the reduction of PtO to Pt, and the peak A6 corresponds to the oxidation of Pt. The peaks C4 and C5 correspond to the reduction of a monolayer of adsorbed hydrogen ions, while the peaks A1 and A2 correspond to its oxidative desorption.

In the voltammogram of cycle 1 (Figure 4b), two reductive peaks C2 and C3 appear at 0.27 V and 0.11 V respectively. Because the cycle 1 is scanned from the OCV where the current is zero, the peak C2 should be regarded as the reductive peak of the adsorbed oxygen  $\text{O}_{\text{chem}}$  on Pt substrate to  $\text{H}_2\text{O}$ . This assumption is accordant with the literatures (WU, 2000: 3683; HERRERO, 1994: 101; FELIU, 1988: 149), in which the results showed that the irreversibly adsorbed Sb species cannot reach a full coverage on the Pt electrode. In other words, the Sb species cannot replace all the  $\text{O}_{\text{chem}}$  on the Pt electrode, so the reductive peak of  $\text{O}_{\text{chem}}$  can still be observed. At the end of cycle 1, the potential is scanned to a very positive potential (1.06 V), where all the  $\text{O}_{\text{chem}}$  will form the oxide PtO with Pt (JERKIEWICZ, 2004: 1451). That is why from cycle 2, only the peak C1 which corresponds to the reduction of PtO to Pt can be observed. The peak C3 should correspond to the reduction of adsorbed  $\text{SbO}^+$  to metallic Sb atoms,

while the peaks A3, A4 and A5 are the oxidative peaks of Sb atoms back to  $\text{SbO}^+$  species. It is worthwhile to note that when the Sb atoms are just oxidized to  $\text{SbO}^+$ , the  $\text{SbO}^+$  species will still adsorb on the Pt substrate, but not desorb (or strip) into the solution if the potential is not extremely positive. This is also the point by which the irreversible adsorption distinguishes from UPD (JUNG, 1997: 277). The observation of the peak C3 and its oxidative peaks is similar as the results reported in the literature (WU, 2000: 3683).

In addition, in the voltammogram of the cycle 1, one can see that the peak C5 is almost completely inhibited and the current intensity of the peak C4 is very low. The inhibition of the reduction of adsorbed hydrogen ions should be attributed to the covered Sb atoms, which occupy a part of sites on Pt electrode. When the scan is performed from the cycle 2 to the cycle 7, the voltammograms show that the peak C3 and A5 decreases greatly, and the oxidative peaks A3 and A4 disappear completely, indicating the amount of the adsorbed Sb species on the surface of Pt substrate decreases. The reason should be that in the end of cycle 1, the very high potential (1.06 V) leads to the desorption of  $\text{SbO}^+$  species. As mentioned above, when the Sb atoms are just oxidized to  $\text{SbO}^+$ , the  $\text{SbO}^+$  species will still adsorb on the Pt substrate, but not strip into the solution. However, the adsorbed  $\text{SbO}^+$  species cannot stand the extremely positive potential such as 1.06 V, where the strong electric field make the positively charged  $\text{SbO}^+$  species desorb into the solution. In addition, the continuously increase of the peaks C4/A2 and C5/A1 also indicates the amount of adsorbed Sb species decreases on the surface of Pt substrate, because there are more and more sites available on Pt electrode for hydrogen adsorption.

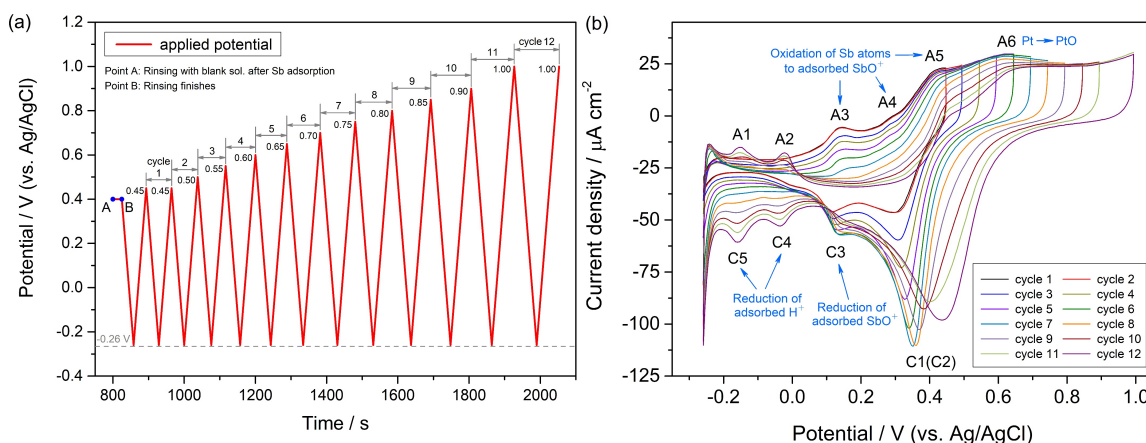


Figure 5: The cyclic voltammetry experiment of the Pt electrode (adsorbed with Sb species) in blank solution: (a) the experimental process and (b) the results of CV scanning. The scanning rate is 20 mV/s.

To confirm the assumption that the decrease of the adsorbed Sb species amount on the surface of Pt substrate is due to the desorption of adsorbed  $\text{SbO}^+$  at a very positive potential, another cyclic voltammetry experiment is performed as follows, and for the sake of clarity, this experimental process is also shown as Figure 5a.

(i) After the irreversible adsorption process of  $\text{SbO}^+$  species is achieved on the Pt electrode, the cell is rinsed with blank solution for 25 s (from point A to B in Figure 5a), and during this time no potential is applied, the voltage showed between point A and B is the OCV. (ii) A cyclic voltammetry scanning is performed for 12 cycles with the same cathodic scanning limit  $-0.26$  V but different anodic scanning limits.

Figure 5b shows the voltammograms of the Pt electrode (adsorbed with Sb species) in blank solution with different anodic scanning limits. One can see that the voltammograms of the cycle 1 and the cycle 2 are highly coincident with each other, illustrating that at the potential of 0.45 V, i.e. the anodic scanning limit of the cycle 1, the  $\text{SbO}^+$  species that are formed by oxidation of metallic Sb can still adsorb on the surface of Pt electrode without stripping. The peaks A3, A4 and A5 start to reduce from the cycle 3 to cycle 12, suggesting that when the potential is equal or more positive than 0.50 V, i.e. the anodic scanning limit of the cycle 2, the adsorbed  $\text{SbO}^+$  species begin to desorb into the solution. When the anodic scanning limit is moved to 1.0 V, the voltammogram of cycle 12 shows that the peak C3 and A5 decreases greatly, and the oxidative peaks A3 and A4 disappear completely, similar to the observation in Figure 4b. In addition, the continuously increase of the peaks C4/A2 and C5/A1 also indicates the amount of the adsorbed Sb species decreases on the surface of Pt substrate from cycle 3 to cycle 12.

The peak C3 seems to increase firstly and then decrease. Actually, this phenomenon is caused by the overlapping with the increasing peak C1 (C2). Along with the anodic scanning limit moving positively, more and more Pt atoms are oxidized to PtO and the amount of the adsorbed oxygen  $\text{O}_{\text{chem}}$  decreases (formed PtO with Pt), so the reductive peak C1 (C2) increases continuously and moves positively, or in other words, the peak C2 evolves to be the peak



C1 during the CV process. Therefore, the peak C3 actually is continually decreasing during the CV process when the overlapping with the peak C1 (C2) is deducted.

The experimental results in Figure 5b prove that the decrease of the amount of adsorbed Sb species on the surface of Pt substrate is due to the desorption of  $\text{SbO}^+$  species at a relatively positive potential. In the corresponding I-t curve of the voltammogram of cycle 2, the total Faradaic charge of the anodic peaks A3, A4 and A5 is integrated to be  $377 \mu\text{C cm}^{-2}$ , i.e. the redox charge of irreversibly adsorbed  $\text{SbO}^+$  species on Pt electrode.

#### UPD of Antimony on a Sb-modified Pt Electrode

The voltammogram of cycle 1 in Figure 4b shows that the reductive current of adsorbed hydrogen does not disappear completely (see peak C4 in Figure 4b), indicating that there are still some unoccupied sites on the surface of Pt electrode after the reduction of the irreversibly adsorbed  $\text{SbO}^+$  to metallic Sb. Therefore, there is chance of further depositing Sb underpotentially on the Pt electrode covered by metallic Sb atoms that are reduced from adsorbed  $\text{SbO}^+$  species. For the sake of convenience, we call the Pt electrode covered by metallic Sb atoms that are reduced from adsorbed  $\text{SbO}^+$  species as Sb-modified Pt electrode. To study the UPD behavior of antimony on a Sb-modified Pt electrode, the experiments are performed as follows, and the corresponding experimental process is also shown as Figure 4a.

(i) After the irreversible adsorption process of  $\text{SbO}^+$  species is achieved on the Pt electrode, the cell is rinsed with blank solution for 25 s (from point A to B in Figure 6a), and during this time no potential is applied, the voltage showed between point A and B is the OCV. (ii) In blank solution, the Pt electrode adsorbed with  $\text{SbO}^+$  species is scanned from the OCV to  $-0.26 \text{ V}$  and then scanned back to  $0.04 \text{ V}$ , and the scanning performed in this step is labelled as cycle 1 (from point B to C in Figure 6a). (iii) The potential of the Pt electrode is remained at  $0.04 \text{ V}$ , while the Sb solution is introduced to the cell and kept flowing for 25 s. (iv) Subsequently, the electrode is scanned from  $0.04 \text{ V}$  to  $-0.26 \text{ V}$  and then scanned back to  $0.45 \text{ V}$ . The scanning performed in this step is labelled as cycle 2. (v) The electrode is scanned from  $0.45 \text{ V}$  to  $-0.26 \text{ V}$  and then scanned back to  $0.45 \text{ V}$ . The scanning performed in this step is labelled as cycle 3. (vi) The potential of the Pt electrode is remained at  $0.45 \text{ V}$ , while the blank solution is introduced again to the cell and kept flowing for 25 s. (vii) In blank solution, the electrode is scanned from  $0.45 \text{ V}$  to  $-0.26 \text{ V}$  and then scanned back to  $0.45 \text{ V}$ . The scanning performed in this step is labelled as cycle 4.

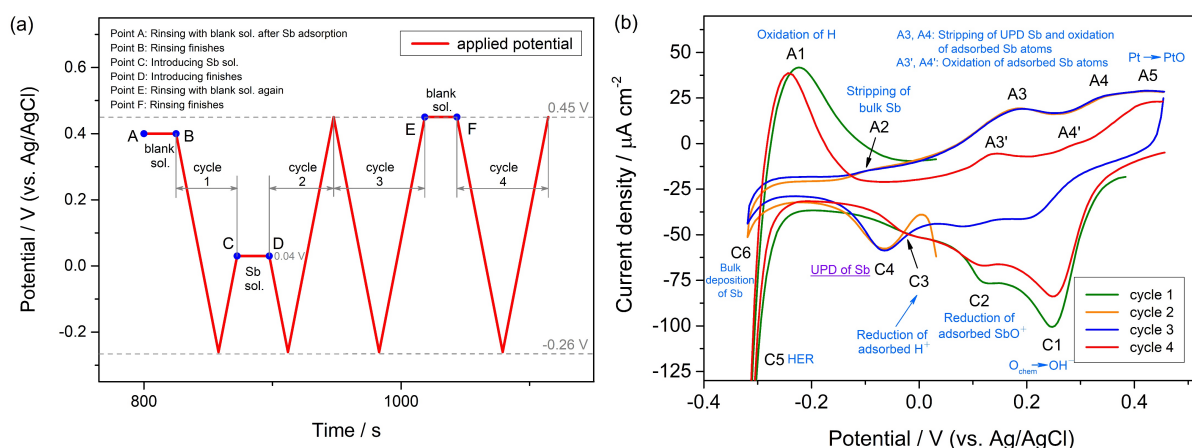


Figure 6: The voltammograms of the Sb-modified Pt electrode in the blank solution and Sb solution (b) and the experimental process (a). Four groups of scanning, cycles 1, 2, 3 and 4, are performed one after another. The cycles 1 and 4 are performed in the blank solution, and the cycles 2 and 3 are performed in the Sb solution. The scanning rate is  $20 \text{ mV/s}$ .

The voltammograms of the cycles 1, 2, 3 and 4 are shown in Figure 6b. For the cycle 1, when the potential moves positively, the scanning is stopped at  $0.04 \text{ V}$ . From Figure 5b one can see that in the anodic branch of the voltammogram of every cycle, when the potential is  $0.04 \text{ V}$ , the peak A2 finishes but the peak A3 does not start, or in other words, the oxidation of the adsorbed hydrogen finishes but the oxidation of the metallic Sb does not begin. Therefore, in cycle 1, when the scanning is stopped at  $0.04 \text{ V}$  in blank solution, all of the hydrogen atoms on the Pt electrode are oxidized but the Sb species can still remain the metallic state. The voltammogram of the cycle 1 is similar as the results shown in Figure 4b and Figure 5b.

Subsequently, the Sb solution is introduced into the cell, while the potential of the electrode is remained at  $0.04 \text{ V}$  during the process of changing solutions. Then the CV scanning of the cycle 2 and cycle 3 are performed successively. In the voltammogram of cycle 2, a new reductive peak C4 is observed at  $-0.07 \text{ V}$ , which corresponds to the UPD of Sb on the Pt electrode. The oxidative peaks A3 and A4 increase obviously and the increased parts should be attributed to the oxidative stripping of the UPD Sb. It is worthwhile to note that the peaks C3 in the CV

curves of cycle 2 and cycle 3 nearly disappear, indicating that there is almost no site available for the adsorption of H species. This observation also suggests a higher coverage of Sb monolayer. In addition, in cycle 1 the peak C5 corresponds to the generation of hydrogen, and A1 is the oxidative peak of the peak C5. However, the peak C5 and A1 cannot be observed in the curves of cycle 2 and cycle 3, but a new pair of redox peaks C6 and A2 appears, which corresponds to the bulk deposition of Sb and its oxidative stripping, respectively.

To confirm that the peak C4 is the UPD peak of Sb and the increased parts of the peaks A3 and A4 correspond to its oxidative stripping, after the scanning of cycle 3 finishes, the cell is rinsed by the blank solution and then the scanning of cycle 4 is performed. Dramatically, the voltammogram of cycle 4 in Figure 6b shows that the peak C4 disappears and the peaks A3 and A4 decrease to the similar intensity as the ones in the curve of cycle 1 in Figure 5b. In addition, the peaks C3, C5 and A1 reappear, but the peaks C6 and A2 cannot be observed. As mentioned above, distinct from the irreversibly adsorbed Sb species, when the UPD Sb atoms are oxidized to  $\text{SbO}^+$  ions, these formed  $\text{SbO}^+$  ions will directly dissolve into the solutions. Thus, during the process of rinsing with the blank solution after cycle 3 at 0.45 V, the UPD Sb will be oxidized to  $\text{SbO}^+$  ions which will be rinsed out of the cell. However, the  $\text{SbO}^+$  species that come from the irreversible adsorption will still adsorb on the surface of the Pt electrode, because the results in Figure 5b prove that the irreversibly adsorbed  $\text{SbO}^+$  species will not desorb at the potential 0.45 V. As a result, when the potential is scanned negatively in cycle 4, there is no  $\text{SbO}^+$  ion existing in the solution. Therefore, the disappearance of the peak C4 and the decrease of the peaks A3 and A4 illustrate that they are related to the UPD of Sb. The Faradic charge of UPD Sb is calculated to be  $604 \mu\text{C cm}^{-2}$  by integrating the increased parts of the peaks A3 and A4 in the corresponding I-t curve of cycle 4. Combined with the reductive charge of irreversibly adsorbed  $\text{SbO}^+$  species, which is  $377 \mu\text{C cm}^{-2}$ , finally a Sb monolayer with the depositing charge  $981 \mu\text{C cm}^{-2}$  is obtained.

#### 4. CONCLUSIONS

Voltammetry and coulometry experiments were performed in this work to investigate the electrochemical behaviors of selenium and antimony on the polycrystalline platinum electrode. The following conclusions were obtained:

(i) Comparing with the results obtained on Au substrates, Se element has different UPD behaviors on Pt substrates. On Pt substrates Se ions can directly form a UPD layer with full coverage, and the total Faradaic charge of the UPD Se is calculated to be  $924 \mu\text{C cm}^{-2}$ . (ii) A Pt electrode adsorbed irreversibly with  $\text{SbO}^+$  species is obtained by introducing the fresh Sb solution continuously into the electrochemical cell. The irreversibly adsorbed  $\text{SbO}^+$  species begin to desorb when the potential is more positive than 0.50 V. The reduction potential of irreversibly adsorbed  $\text{SbO}^+$  to metallic Sb atoms amounts to 0.11 V and the Faradic charge of this process is integrated to be  $377 \mu\text{C cm}^{-2}$ . (iii) After the irreversibly adsorbed  $\text{SbO}^+$  species are reduced to metallic Sb, Sb atoms can be further deposited onto this Sb-modified Pt electrode in the way of UPD to increase the coverage of the metallic Sb monolayer. The UPD potential of antimony on the Sb-modified Pt electrode amounts to  $-0.07 \text{ V}$ . The Faradic charge of UPD Sb is calculated to be  $604 \mu\text{C cm}^{-2}$ . (iv) Combined with the reductive charge of irreversibly adsorbed  $\text{SbO}^+$  species, finally a Sb monolayer with the depositing charge  $981 \mu\text{C cm}^{-2}$  is obtained. Now the alternative deposition of Sb-Se compound by EC-ALE method is under study.

#### Acknowledgements

The authors gratefully acknowledge the financial support for this work from Hubei Provincial Key Laboratory of Green Materials for Light Industry (201710A06) and Chutian Scholars Program of the Hubei Province of China.

#### 5. REFERENCES

- CHEN Y, 2014. A voltammetric study of the underpotential deposition of cobalt and antimony on gold. *Journal of Electroanalytical Chemistry*, 724 (19), 55.
- CHEN Y, 2015. Underpotential deposition of selenium and antimony on gold. *Journal of Solid State Electrochemistry*, 19(8), 2399.
- FELIU JM, 1988. ChemInform abstract: new observations of a structure sensitive electrochemical behavior of irreversibly adsorbed arsenic and antimony from acidic solutions on Pt (111) and Pt (100) orientations. *Journal of Electroanalytical Chemistry*, 256 (1), 149.
- FERNÁNDEZ AM, 2000. Preparation and characterization of  $\text{Sb}_2\text{Se}_3$  thin films prepared by electrodeposition for photovoltaic applications. *Thin Solid Films*, 366 (1), 202.
- FLOWERS JR, 2002. Atomic layer epitaxy of CdTe using an automated electrochemical thin-layer flow deposition reactor. *Journal of Electroanalytical Chemistry*, s524-525 (02), 273.

---

FORESTI ML, 2005. Ternary  $\text{CdS}_x\text{Se}_{1-x}$  deposited on Ag (111) by ECALE: synthesis and characterization. *Langmuir the ACS Journal of Surfaces & Colloids*, 21 (15), 6900.

GHOSH G, 1994. The Sb-Te (antimony-tellurium) system. *Journal of Phase Equilibria*, 15 (3), 349.

GREGORY B, 1991. Electrochemical atomic layer epitaxy (ECALE). *Journal of Electroanalytical Chemistry & Interfacial Electrochemistry*, 1991, 300 (91), 543.

HERRERO E, 1994. Poison formation reaction from formic acid on Pt (100) electrodes modified by irreversibly adsorbed bismuth and antimony. *Journal of Electroanalytical Chemistry*, 368 (1-2), 101.

JERKIEWICZ G, 2004. Surface-oxide growth at platinum electrodes in aqueous  $\text{H}_2\text{SO}_4$ : reexamination of its mechanism through combined cyclic-voltammetry, electrochemical quartz-crystal nanobalance and Auger electron spectroscopy measurements. *Electrochimica Acta*, 49 (9), 1451.

JUNG G, 1997. Two electrochemical processes for the deposition of Sb on Au (100) and Au (111): irreversible adsorption and underpotential deposition. *Journal of Electroanalytical Chemistry*, 436 (1-2), 277.

KIZHAKEVARIAM N, 1994. Structure and reactivity of bimetallic electrochemical interfaces: infrared spectroscopic studies of carbon monoxide adsorption and formic acid electrooxidation on antimony-modified Pt (100) and Pt (111). *Surface Science*, 310 (1-3), 183.

LISTER TE, 1996. Formation of the first monolayer of CdSe on Au (111) by electrochemical ALE. *Applied Surface Science*, 107 (107), 153.

MADELUNG O, 1992. Semiconductors: other than group IV elements and III-V compounds. Germany: Springer-Verlag.

RAJPURE KY, 1999. A comparative study of the properties of spray-deposited  $\text{Sb}_2\text{Se}_3$  thin films prepared from aqueous and nonaqueous media. *Materials Research Bulletin*, 34 (7), 1079.

SANTOS MC, 2004. Microgravimetric, rotating ring-disc and voltammetric studies of the underpotential deposition of selenium on polycrystalline platinum electrodes. *Journal of Electroanalytical Chemistry*, 567 (2), 203.

SUN SG, 1990. Electrocatalytic properties of glassy metals: combined auger electron spectroscopy and electrochemical studies of the surface composition and electrocatalysis of CO oxidation at amorphous  $\text{Pt}_{66}\text{Sb}_{34}$  alloy. *Journal of Electroanalytical Chemistry*, 278 (1-2), 205.

TRASATTI S, 1991. Real surface area measurement in electrochemistry. *Pure & Applied Chemistry*, 63 (5), 353.

WANG X, 2013. Preparation and electrical transport properties of nanostructured  $\text{Sb}_2\text{Se}_3$  films fabricated by combining spin-coating and gas-induced reduction. *Journal of Nanoparticle Research*, 15 (4), 1.

WU QH, 2000. An EQCM study of Sb adsorption and coadsorption with CO on Pt electrode in perchloric acid solutions. *Electrochimica Acta*, 45 (22-23), 3683.

XIAO CJ, 2009. Electrodeposition and characterization of  $\text{Bi}_2\text{Se}_3$  thin films by electrochemical atomic layer epitaxy (ECALE). *Electrochimica Acta*, 54 (27), 6821.

XIAO XB, 2006. Thermoelectrics handbook: macro to nano. Boca Raton: CRC.

YAN JW, 2004. Electrodeposition of Sb on Au (100) at underpotentials: structural transition involving expansion of the substrate surface. *Electrochemistry Communications*, 6 (8), 843.

YANG JY, 2006. Formation and characterization of  $\text{Sb}_2\text{Te}_3$  nanofilms on Pt by electrochemical atomic layer epitaxy. *Journal of Physical Chemistry B*, 110 (10), 4599.

YU L, 2010. Pulsed laser deposited heterogeneous mixture of  $\text{Li}_2\text{Se}-\text{Sb}_2\text{Se}_3$  nanocomposite as a new storage lithium material. *Electrochimica Acta*, 55 (3), 1258.

---

XUE MZ, 2008. Pulsed laser deposited  $\text{Sb}_2\text{Se}_3$  anode for lithium-ion batteries. *Journal of Alloys & Compounds*, 458 (1), 351.

ZHU W, 2005. Effect of potential on bismuth telluride thin film growth by electrochemical atomic layer epitaxy. *Electrochimica Acta*, 50 (20), 4041.

ZHU W, 2005. The underpotential deposition of bismuth and tellurium on cold rolled silver substrate by ECALE. *Electrochimica Acta*, 50 (27), 5465.